

New scenarios for hard-core interactions in a hadron resonance gas

L. M. Satarov,^{1,2} V. Vovchenko,^{1,3,4} P. Alba,¹ M. I. Gorenstein,^{1,5} and H. Stoecker^{1,3,6}

¹ *Frankfurt Institute for Advanced Studies,
D-60438 Frankfurt am Main, Germany*

² *National Research Center "Kurchatov Institute" 123182 Moscow, Russia*

³ *Institut für Theoretische Physik, Goethe Universität Frankfurt,
D-60438 Frankfurt am Main, Germany*

⁴ *Department of Physics, Taras Shevchenko
National University of Kiev, 03022 Kiev, Ukraine*

⁵ *Bogolyubov Institute for Theoretical Physics, 03680 Kiev, Ukraine*

⁶ *GSI Helmholtzzentrum für Schwerionenforschung GmbH, D-64291 Darmstadt, Germany*

Abstract

The equation of state of a baryon-symmetric hadronic matter with hard-sphere interactions is studied. It is assumed that mesons M are point-like, but baryons B and antibaryons \bar{B} have the same hard-core radius r_B . Three possibilities are considered: 1) the BB and $B\bar{B}$ interactions are the same; 2) baryons do not interact with antibaryons; 3) the $B\bar{B}$, MB , and $M\bar{B}$ interactions are negligible. By choosing the parameter $r_B = 0.3 - 0.6$ fm, we calculate the nucleon to pion ratio as a function of temperature and perform the fit of hadron yields measured in central Pb+Pb collisions at $\sqrt{s_{NN}} = 2.76$ TeV. New nontrivial effects in the interacting hadron resonance gas at temperatures 150 – 200 MeV are found.

PACS numbers: 24.10.Pa, 25.75.-q, 21.65.Mn

I. INTRODUCTION

The equation of state (EoS) and the phase diagram of the strongly interacting matter are in the focus of high-energy heavy-ion collisions and in astrophysics. Some information on infinite equilibrium systems has been obtained from lattice QCD calculations [1, 2]. However, that approach has not yet been developed for large baryon chemical potentials and for small temperatures. The EoS in this domain is still rather uncertain. Phenomenological models of phase transitions in nuclear matter show [3, 4] that a realistic phase diagram cannot be obtained without an explicit account of the hadronic interactions.

Since the beginning of the 1980ies several thermal models were constructed [5–9] to describe yields of secondary hadrons in relativistic nuclear collisions. These model assume that such particles are emitted from a statistically equilibrated system with an ideal gas EoS. The temperature T and baryon chemical potential μ_B of the emitting source were found by fitting the observed yields of stable hadrons. Many experimental data have been reproduced within this approach. On the other hand, simple estimates show that hadron densities at the chemical freeze-out stage of the reaction are rather large, therefore, one can expect significant deviations from the ideal gas picture.

The hard-sphere interaction is one of the most popular approximations for implementing short-range repulsion in multiparticle systems, both in molecular and nuclear physics. It is assumed that particles move freely unless the distance between their centers equals the sum of their hard-core radii. This approximation was suggested by van der Waals for describing properties of dense gases and liquids. Similar ‘excluded volume’ models were applied [3, 10] to study the effects of short-range interactions in hadronic systems. Early versions of this model chose the same hard-core radius [4, 11, 12] for all hadronic species. Attempts to introduce different radii for different kinds of hadrons have been made in Refs. [13–17]. Later on, more refined versions of the excluded volume approach were developed which agree well with the virial expansion [18] for systems with the hard-sphere interaction. In particular, the Carnahan-Starling (CS) approximation [19] have been applied in [20, 21]. As demonstrated in Ref. [20], superluminal sound velocities appear in the CS approach only at very high energy densities, where the deconfinement effects become important.

There is another problem disregarded in existing excluded volume calculations. They implicitly assume that antibaryons \overline{B} interact with baryons B in the same way as the baryon-

baryon pairs. On the other hand, there are arguments [22] that the $B\bar{B}$ interactions should be less repulsive than those for BB pairs. Up to now not much is known about the $B\bar{B}$ and meson-(anti)baryon short-range interactions. Below it is assumed that mesons M are point-like (with vanishing hard-core) and all (anti)baryons have the same hard-core radii. Three possible scenarios are considered: 1) the BB and $B\bar{B}$ interactions are the same; 2) baryons do not interact with antibaryons; 3) the $B\bar{B}$, MB , and $M\bar{B}$ interactions are neglected. As far as we know, we are the first who takes into account possible difference of the BB and $B\bar{B}$ interactions in the excluded volume approach.

Most calculations in this paper are done for baryon-symmetric matter with equal numbers of baryon and antibaryons, i.e. assuming $\mu_B = 0$. Presumably, such matter is formed in nuclear collisions at the LHC energies. Using the above mentioned models with the full set of known hadrons, we fit the midrapidity hadron yields observed by the ALICE Collaboration in central Pb+Pb collisions at $\sqrt{s_{NN}} = 2.76$ TeV. In agreement with Ref. [17] we show that χ^2/N_{dof} values for all our fits are much broader functions of temperature as compared to the ideal gas calculations.

We found strong effects of hadron short-range interactions in the high temperature region. It is shown that at $\mu_B = 0$, the nucleon to pion ratio as a function of temperature has a maximum in the interval $T = 150 - 200$ MeV. The position and height of this maximum are model dependent. In particular, they are rather sensitive to omitting the $B\bar{B}$ repulsion. We apply the same models to study the temperature dependence of the pressure. These results are compared to lattice QCD calculations.

This paper is organized as follows. In Sec. II we introduce different schemes to study the effects of the hard-core repulsion in a one-component gas as well as in a multi-component system of hadrons. In Sec. III we present numerical results for a baryon-symmetric system containing the full set of known hadrons. Attention is paid to calculating the nucleon to pion ratio. The results for pressure as a function of temperature are also presented and compared with lattice QCD data. Sec. IV presents our fits to the hadron yields measured by the ALICE Collaboration. The conclusions and an outlook are presented in Sec. V. Appendices A, B and C provide formulae for calculating thermodynamic functions in the grand canonical variables.

II. HARD CORE REPULSION IN HADRON GAS

In the Boltzmann approximation the ideal gas pressure P^{id} in the grand canonical ensemble (GCE) can be written as ($\hbar = c = 1$)

$$P^{\text{id}}(T, \{\mu\}) = T \sum_i n_i^{\text{id}}(T, \mu_i), \quad n_i^{\text{id}}(T, \mu_i) = \exp\left(\frac{\mu_i}{T}\right) \phi_i(T), \quad \phi_i(T) = \frac{g_i m_i^2 T}{2\pi^2} K_2\left(\frac{m_i}{T}\right), \quad (1)$$

where T is the system temperature, μ_i and n_i^{id} denote, respectively, the chemical potential and the ideal gas number density of i th hadron species, m_i and g_i are, respectively, the i th hadron mass and statistical weight, $K_2(x)$ is the McDonald function. The function $\phi_i(T)$ denotes the ideal gas density of i th hadrons at $\mu_i = 0$. Note that we apply the zero-width approximation to find contributions of hadronic resonances.

In this paper we study the equilibrium system composed of hadrons with the hard-core repulsion. Different schemes for taking into account these interactions are considered. First, the one-component gas is studied, and then the multi-component mixtures of hadron species will be discussed.

To illustrate the physical effects in different model formulations we first consider a simple system of nucleons N , antinucleons \bar{N} , and pions π at temperature T and the baryon chemical potential $\mu_B = 0$. This example will be used to study qualitatively the role of short-range repulsive interactions in the hadronic system which includes simultaneously mesons and baryon-antibaryon pairs. In the considered case the chemical potentials of all hadrons vanish, $\mu_i = 0$ ($i = N, \bar{N}, \pi$), and the densities of antinucleons and nucleons coincide, $n_{\bar{N}} = n_N$. In these calculations we assume that nucleons have a finite hard-core radius r_N and pions are point-like, i.e. $r_\pi = 0$.

A. One-component gas of hard spheres

In this subsection we consider the EoS of a single-component system with the hard-sphere interaction of particles. Let us denote by r the hard-core radius of the particle. In the Boltzmann approximation, one can write the following 'exact' expression for the pressure [23]:

$$P = nTZ(\eta). \quad (2)$$

Here n is the number density of particles, $\eta = nv$ denotes their "packing" fraction, where $v = 4\pi r^3/3$ is a single-particle hard-core eigenvolume. The dimensionless "compressibility" factor $Z(\eta)$ does not depend on temperature. It is clear that $Z(\eta) \rightarrow 1$ in the ideal gas limit $\eta \rightarrow 0$. Note that Eq. (2) is valid for packing fractions below the critical value of the liquid-solid transition $\eta_c \simeq 0.49$ [23].

Different authors either use numerically tabulated values of $Z(\eta)$ or apply analytical approximations. The simple van der Waals excluded volume approximation,

$$Z_{\text{EV}}(\eta) = (1 - 4\eta)^{-1} = 1 + 4\eta + 16\eta^2 + \dots, \quad (3)$$

is used in the eigenvolume (EV) models. The approximation (3) correctly describes the second term of the virial expansion for the pressure [18], but it fails to reproduce higher-order terms which give the contribution of non-binary interactions. A comparison with numerical calculations shows that Eq. (3) strongly overestimates the values of $Z(\eta)$ at $\eta \gtrsim 0.2$ [20]. Note that values $\eta > 0.25$ are not allowed in this model.

A very accurate and relatively simple approximation was suggested [19] by Carnahan and Starling (CS). It has the form

$$Z_{\text{CS}}(\eta) = \frac{1 + \eta + \eta^2 - \eta^3}{(1 - \eta)^3} = 1 + 4\eta + 10\eta^2 + \dots. \quad (4)$$

Note, that the third term of the virial expansion for $Z(\eta)$ is correctly reproduced within the CS model. It is interesting that Eq. (4) reproduces rather accurately the virial expansion terms up to the eighth order [23]. In fact, this approximation can be safely used in the whole domain $\eta < \eta_c$. One can see that $Z_{\text{CS}}(\eta) \simeq Z_{\text{EV}}(\eta)$ at small η .

The above equations correspond to the canonical ensemble (CE). The transformation to the GCE can be done using the following procedure. Integrating Eq. (2) over the system volume one obtains the free energy density $f = f(T, n)$ (see Appendix A). Using the thermodynamical relation $\mu = (\partial f / \partial n)_T$, one finds the transcendental equation for the GCE particle density $n = n(T, \mu)$

$$n = n^{\text{id}}[T, \mu - T\psi(vn)], \quad (5)$$

where $n^{\text{id}}(T, \mu)$ is given by the second equality of (1) with the replacement $\mu_i \rightarrow \mu$. The dimensionless function

$$\psi(\eta) = Z(\eta) - 1 + \int_0^\eta \frac{d\eta'}{\eta'} [Z(\eta') - 1] \quad (6)$$

describes the shift of chemical potential (in units of T) for a one-component matter with hard-sphere interactions as compared to the ideal gas [24]. Finally, the GCE pressure is calculated by substituting the solution of (5) into Eq. (2).

Within the EV and CS models one can calculate the function $\psi(\eta)$ analytically. Substituting (3) and (4) into Eq. (6) gives¹

$$\psi_{\text{EV}}(\eta) = \frac{4\eta}{1-4\eta} - \ln(1-4\eta) = 8\eta + 24\eta^2 + \dots, \quad (7)$$

$$\psi_{\text{CS}}(\eta) = \frac{3-\eta}{(1-\eta)^3} - 3 = 8\eta + 15\eta^2 + \dots. \quad (8)$$

An equivalent GCE formulation of the EV model was obtained earlier in Ref. [3].

B. Diagonal eigenvolume model

A simple extension of the EV model for multi-component systems was suggested in Ref. [11]. The pressure of a hadronic mixture is parameterized as

$$P = T \sum_i \xi_i, \quad \xi_i = \frac{n_i}{1 - \sum_j b_j n_j}, \quad (9)$$

where $b_i = 16\pi r_i^3/3$ and n_i are, respectively, the eigenvolume parameter and the density of i th hadrons. The sums in Eq. (9) go over all types of hadrons. Following Ref. [17], we denote this excluded volume scheme as the "diagonal" eigenvolume model (DEM).

Calculating the free energy density of the hadronic mixture and taking its derivatives with respect to n_i (see Appendix A), one finds the following equation for the chemical potential of i th particles:

$$\mu_i = T \ln \frac{\xi_i}{\phi_i(T)} + b_i P, \quad (10)$$

where ξ_i and P are taken from Eq. (9). In fact, the above equation provides the transition from the CE to the GCE. Using Eq. (1) one can rewrite (10) in the equivalent form

$$\xi_i = n_i^{\text{id}}(T, \mu_i - b_i P). \quad (11)$$

Substituting (11) into Eq. (9) gives the transcendental equation for the pressure [11]

$$P = \sum_i P_i^{\text{id}}(T, \mu_i - b_i P), \quad (12)$$

¹ Note that $\psi_{\text{CS}}(\eta) < \psi_{\text{EV}}(\eta)$ at $\eta < 0.25$.

and allows to calculate the particle number densities

$$n_i = \frac{\xi_i}{1 + \sum_j b_j \xi_j}. \quad (13)$$

Equations (11) and (13) lead to the following expressions for density ratios of different hadronic species:

$$\frac{n_i}{n_j} = \frac{n_i^{\text{id}}}{n_j^{\text{id}}} \exp \left[(b_j - b_i) \frac{P}{T} \right]. \quad (14)$$

The ratio (14) is smaller than that of the ideal gas if $b_i > b_j$.

For the $N\bar{N}\pi$ mixture with $\mu_N = \mu_{\bar{N}} = \mu_\pi = 0$ and "point-like" pions ($r_\pi = 0$) one can represent Eq. (12) in the form

$$P = T \left[2\phi_N(T) \exp \left(-\frac{b_N P}{T} \right) + \phi_\pi(T) \right]. \quad (15)$$

Note that the second term on the right hand side (r.h.s.) of this equation gives the partial pressure of pions which is not suppressed as compared to the ideal pion gas. Equation (13) yields the following expressions for the hadronic densities:

$$n_N = \frac{\xi_N}{1 + 2b_N \xi_N}, \quad n_\pi = \frac{\phi_\pi(T)}{1 + 2b_N \xi_N}, \quad (16)$$

where $\xi_N = \phi_N(T) \exp(-b_N P/T)$. Finally, we arrive at the equation for the nucleon-to-pion ratio

$$\frac{N}{\pi} \equiv \frac{n_N}{n_\pi} = \frac{\phi_N(T)}{\phi_\pi(T)} \exp \left(-\frac{b_N P}{T} \right), \quad (17)$$

where P is determined by solving Eq. (15). Note that (17) is a particular case of Eq. (14).

Figure 1 shows N/π ratio in the DEM for different values of r_N from 0.3 to 0.5 fm. This ratio is a non-monotonic function of T with a maximum in the temperature range between about 200 to 300 MeV. Note the same N/π ratio is reproduced by two different values of T . The higher temperature value corresponds to a denser state of the $N\bar{N}\pi$ matter with stronger short-range interactions of hadrons. It should be noted that this simple $N\bar{N}\pi$ system is considered here for illustration. Hadronic states of higher masses will be introduced below. One should also have in mind the appearance of the crossover transition to the deconfined quark-gluon plasma at high temperatures.

At temperatures $m_\pi \lesssim T \ll m_N$ the following approximate relations hold (see Eq. (1)):

$$\phi_N(T) \simeq \frac{1}{2} \left(\frac{2m_N T}{\pi} \right)^{3/2} \exp \left(-\frac{m_N}{T} \right), \quad \phi_\pi(T) \simeq \frac{3}{\pi^2} T^3, \quad (18)$$

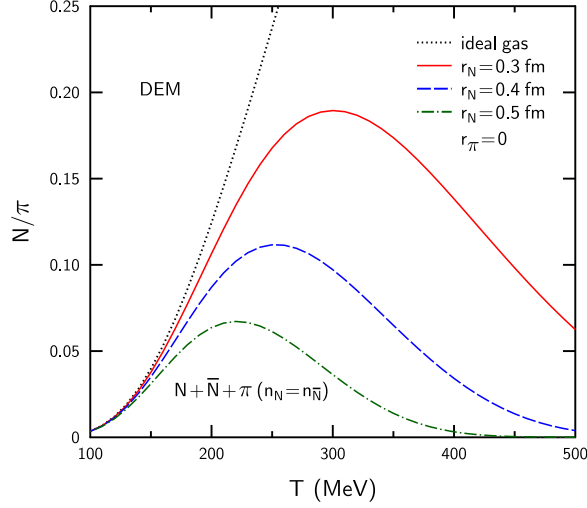


FIG. 1: (Color online) The N/π ratio as a function of temperature in the $N\bar{N}\pi$ matter with point-like pions and equal numbers of nucleons and antinucleons. The solid, dashed, and dash-dotted lines correspond to nucleon hard-core radii $r_N = 0.3, 0.4$ and 0.5 fm, respectively. The dotted line is obtained in the ideal gas limiting case $r_N = 0$.

Substituting (18) into (17) gives

$$\frac{n_N}{n_\pi} \simeq \frac{\sqrt{2\pi}}{3} \left(\frac{m_N}{T} \right)^{3/2} \exp[-\varphi(T)], \quad (19)$$

where

$$\varphi(T) = \frac{m_N + b_N P}{T} \simeq \frac{m_N}{T} + \frac{3b_N T^3}{\pi^2}. \quad (20)$$

The last estimate is obtained by neglecting the first term in Eq. (15). This is a reasonable approximation at the temperatures considered here. The temperature dependence of n_N/n_π is determined mainly by the last factor in Eq. (19). As one can see from Eq. (20), it is a non-monotonic function of T with a maximum at $T \simeq \left(\frac{\pi^2 m_N}{9 b_N} \right)^{1/4}$. The calculation shows that the maximum is shifted from about 350 to 250 MeV when r_N increases from 0.3 to 0.5 fm. This agrees with the numerical results shown in Fig. 1. As will be shown in Sec. III, the inclusion of heavier hadrons and resonances reduces the N/π ratio and shifts the maxima to lower temperatures.

C. Non-diagonal eigenvolume model

The DEM considered in preceding section is not accurate already in the second order of the virial expansion for classical particles with hard-sphere interactions. Indeed, expanding Eq. (9) in powers of partial densities leads to the relation

$$\frac{P}{T} = \sum_i n_i + \sum_{i,j} b_j n_i n_j + \dots, \quad (21)$$

whereas the virial expansion gives [18]

$$\frac{P}{T} = \sum_i n_i + \sum_{i,j} B_{ij} n_i n_j + \dots, \quad B_{ij} = 2\pi(r_i + r_j)^3/3. \quad (22)$$

One can see that $B_{ij} \neq b_j$ for non-equal hard-core radii, $r_i \neq r_j$.

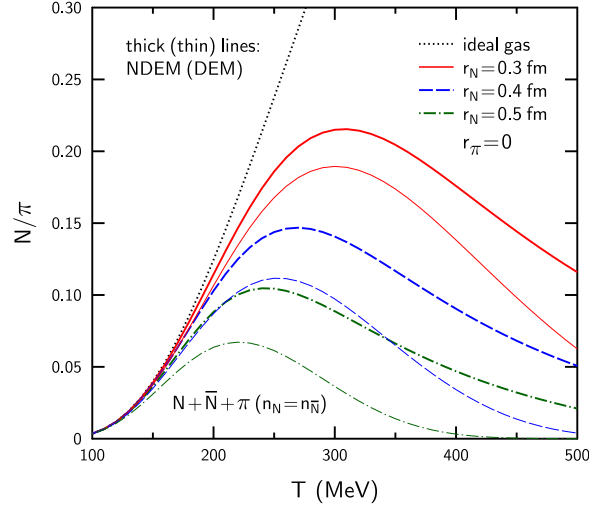


FIG. 2: (Color online) The N/π ratio as a function of temperature in the $N\bar{N}\pi$ matter with equal numbers of nucleons and antinucleons. The thick solid, dashed, and dash-dotted lines are calculated by using the NDEM with nucleon hard-core radii $r_N = 0.3, 0.4$ and 0.5 fm, respectively. Thin lines give corresponding results obtained within the DEM. The dotted line is calculated in the ideal gas limit $r_N = 0$.

In this subsection we consider the EoS of a hadronic mixture by using the improved "non-diagonal" eigenvolume model² (NDEM) suggested in Ref. [13]. This scheme yields agreement with the second-order virial expansion (22).

² It is called the "crossterms" eigenvolume model in Ref. [17].

The pressure in the NDEM is given by Eq. (9) with the replacement b_j by the matrix

$$b_{ij} = \frac{2B_{ij}B_{ii}}{B_{ii} + B_{jj}}. \quad (23)$$

Then one gets the relations

$$P = T \sum_i \xi_i, \quad \xi_i = \frac{n_i}{1 - \sum_j b_{ji} n_j}, \quad (24)$$

Instead of Eqs. (10) and (11), after the transition to the CGE (see Appendix A) one obtains the equations

$$\mu_i = T \left(\ln \frac{\xi_i}{\phi_i(T)} + \sum_j b_{ij} \xi_j \right), \quad (25)$$

which are equivalent to

$$\xi_i = n_i^{\text{id}}(T, \mu_i - T \sum_j b_{ij} \xi_j). \quad (26)$$

Note that in a general case one should explicitly solve the set of coupled equations (26) instead of a single equation (12) in the DEM. At known ξ_i one can calculate the densities n_i by using the second equality in (24). The NDEM is reduced to the DEM if all hard-core radii are equal, $r_i = r_j$, and thus $b_{ij} = b_i$. In this case, the particle number ratios n_i/n_j become equal to their ideal gas values $n_i^{\text{id}}/n_j^{\text{id}}$.

Let us again consider the $N\bar{N}\pi$ system with $\mu_N = \mu_{\bar{N}} = \mu_\pi = 0$ and assume that pions are point-like. Denoting (anti)nucleons and pions by indices '1' and '2', respectively, one can write the relations $b_{11} = 4b_{12} = b_N, b_{22} = b_{21} = 0$. As a result, instead of Eqs. (24) and (26), one obtains³

$$\frac{P}{T} = 2\xi_N + \phi_\pi, \quad (27)$$

$$\xi_N = \phi_N \exp[-b_N(2\xi_N + \phi_\pi/4)], \quad (28)$$

$$n_N = \frac{\xi_N}{1 + 2b_N\xi_N}, \quad n_\pi = \phi_\pi(1 - b_N n_N/2). \quad (29)$$

Solving Eq. (28) with respect to ξ_N , we can calculate P and the number densities n_N, n_π by using Eqs. (27) and (29).

A comparison of the N/π ratios in the NDEM and DEM is shown in Fig. 2. It is seen that at fixed r_N the NDEM predicts larger values of the N/π , which are smaller suppressed

³ One gets the corresponding equations of the DEM after replacing $\phi_\pi \rightarrow 4\phi_\pi$ in Eq. (28) and $n_N \rightarrow 4n_N$ in the second equality of Eq. (29).

as compared to the ideal gas. Below only the NDEM is used, and it is denoted for brevity the ‘eigenvolume model’ (EVM).

D. Binary mixture of hard spheres and point-like particles

In the case of a binary mixture⁴ where particles of one component are point-like, it is possible to apply the CS model (CSM) [20] which is valid at much larger densities than the NDEM.

Let us denote the components of such a binary matter by indices $i = 1, 2$ and assume that particles of the first component interact as hard spheres of the radius r_1 , but particles of the second kind are point-like. In this case, similar to Eq. (2), one can write the equation [23]

$$P = T \left[n_1 Z(\eta_1) + \frac{n_2}{1 - \eta_1} \right]. \quad (30)$$

Here n_i is the number density of the i th component, $\eta_1 = n_1 v_1$ is the ”packing” fraction of the first particles where $v_1 = 4\pi r_1^3/3$ denotes their single-particle (hard-core) eigenvolume. The denominator in the second term in the r.h.s. of Eq. (2) describes the reduction of the volume available for particles $i = 2$.

As shown in Appendix B, Eq. (30) leads to following equations for chemical potentials:

$$\mu_1 = T \left[\ln \frac{n_1}{\phi_1(T)} + \psi(n_1 v_1) + \frac{n_2 v_1}{1 - n_1 v_1} \right], \quad (31)$$

$$\mu_2 = T \left[\ln \frac{n_2}{\phi_2(T)} - \ln(1 - n_1 v_1) \right], \quad (32)$$

where $\psi(\eta)$ is defined in Eq. (6). The first term in the r.h.s. of (31) equals the ideal gas chemical potential μ_1^{id} . The second one gives the shift of μ_1 induced by interactions of the first particles. The last term appears due to interactions of particles $i = 1$ and $i = 2$. It equals the minimal work for creating a cavity with the volume v_1 inside of a gas of point-like particles [20]. The shift of μ_2 is due to reducing the total volume accessible for particles $i = 2$. Using Eqs. (6) and (30)–(32) one can prove the validity of the thermodynamic relation $dP = n_1 d\mu_1 + n_2 d\mu_2$ for an arbitrary isothermal process⁵. Note the the shifts of chemical potentials disappear in the limit $v_1 \rightarrow 0$.

⁴ One may consider the $N\bar{N}\pi$ matter with $n_N = n_{\bar{N}}$ as a binary $N\pi$ mixture with the ’nucleon’ density $2n_N$. However, this is not correct if NN and $N\bar{N}$ interactions are different (see Sec. II E).

⁵ This relation provides the thermodynamic consistency of the model.

In the case of vanishing chemical potentials, $\mu_1 = \mu_2 = 0$, one gets the following relations for the particle densities:

$$n_1 = n_1^{\text{id}} \exp \left[-\psi(n_1 v_1) - n_2^{\text{id}} v_1 \right], \quad (33)$$

$$n_2 = n_2^{\text{id}} (1 - n_1 v_1). \quad (34)$$

Therefore, the problem is reduced to solving Eq. (33) with respect to n_1 .

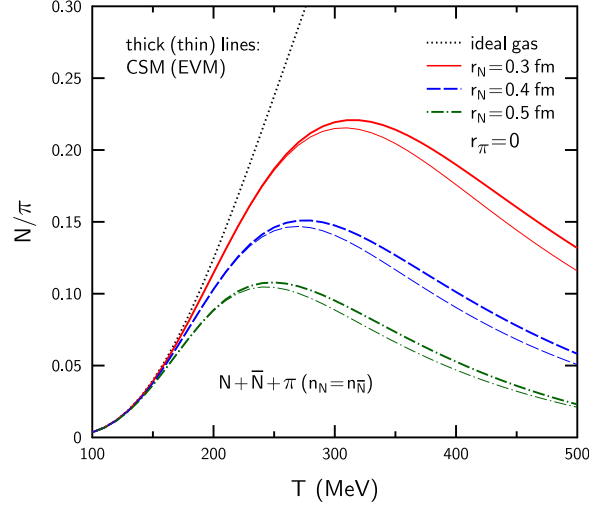


FIG. 3: (Color online) The N/π ratio as a function of temperature in the $N\bar{N}\pi$ matter with equal numbers of nucleons and antinucleons. The thick solid, dashed, and dash-dotted lines are calculated by using the CSM with nucleon hard-core radii $r_N = 0.3, 0.4$ and 0.5 fm, respectively. Thin lines give corresponding results obtained within the EVM. The dotted line is calculated assuming $r_N = 0$.

To determine properties of $N\bar{N}\pi$ matter with $n_N = n_{\bar{N}}$ one should substitute $n_1 = 2n_N$, $n_1^{\text{id}} = 2\phi_N$, $v_1 = v_N = b_N/4$ and make the replacement $n_2 \rightarrow n_\pi$. One then arrives at the equations

$$\frac{P}{T} = 2n_N Z(2n_N v_N) + \phi_\pi, \quad (35)$$

$$n_N = \phi_N \exp \left[-\psi(2n_N v_N) - \phi_\pi v_N \right], \quad (36)$$

$$n_\pi = \phi_\pi (1 - 2n_N v_N). \quad (37)$$

The CSM is obtained by substituting the expressions $Z = Z_{\text{CS}}, \psi = \psi_{\text{CS}}$ from Eqs. (4) and (8), whereas the EVM corresponds to $Z = Z_{\text{EV}}, \psi = \psi_{\text{EV}}$ given by Eqs. (3) and (7). In the latter case the above equations are equivalent to Eqs. (27)–(29) of the NDEM.

As mentioned above, $\psi_{\text{CS}}(\eta) < \psi_{\text{EM}}(\eta)$. According to Eqs. (36) and (37), this implies that the inequalities $n_N^{(\text{CSM})} > n_N^{(\text{EVM})}$ and $n_\pi^{(\text{CSM})} < n_\pi^{(\text{EVM})}$ hold at fixed T and r_N . Therefore, the N/π ratio should be larger in the CSM as compared to the EVM.

Such a conclusion is confirmed by the results of numerical calculations shown in Fig. 3. However, one can see that the difference between the CSM and EVM results is not very significant. This follows from relatively small packing fractions for (anti)nucleons ($\eta = 2n_N v_N \lesssim 0.1$) in the $N\bar{N}\pi$ matter at $\mu_B = 0$. It will be shown below that a similar situation occurs after inclusion of hadronic resonances. Note, that much larger baryon densities may be achieved in baryon-asymmetric systems with nonzero μ_B [4].

E. The $N\bar{N}\pi$ matter without $N\bar{N}$ interactions

Up to now it was assumed that antinucleons interact with nucleons as hard spheres of the same radii, i.e. we did not introduce any differences between the $N\bar{N}$ and NN interactions. However, due to the G-parity symmetry, the vector part of the $N\bar{N}$ pair potential has an opposite sign as compared to the NN one [22]. As a consequence, the $N\bar{N}$ interaction should be less repulsive at short distances than that for NN pairs⁶. Another reason for reduced short-range repulsion is the Pauli exclusion principle which should be less restrictive for $N\bar{N}$ interactions. Possibility of vanishing short-range repulsion between baryons and antibaryons has been pointed out in Ref. [26].

To study the sensitivity to the asymmetry between the $N\bar{N}$ and NN interactions, we consider below the EoS of the $N\bar{N}\pi$ matter assuming a totally vanishing repulsion for $N\bar{N}$ pairs. In this case the nucleon and antinucleon components of the $N\bar{N}\pi$ system become mutually independent. It is not difficult to modify the "binary mixture" EoS for the case of $N\bar{N}\pi$ matter without the $N\bar{N}$ interaction. Instead of the first term in Eq. (30) we take the sum of two contributions from purely nucleon and antinucleon fluids:

$$(n_N + n_{\bar{N}})Z(n_N v_N + n_{\bar{N}} v_N) \rightarrow n_N Z(n_N v_N) + n_{\bar{N}} Z(n_{\bar{N}} v_N).$$

Using further the procedure analogous to that used in Sec. IID one gets the equations which differ from Eqs. (35)–(37) by the replacement $2n_N v_N \rightarrow n_N v_N$ in the arguments of

⁶ Motivated by these features, we introduced in [25] an attractive vector field for antibaryons in nuclear matter, predicting strong binding and compression effects for antibaryon-doped nuclei.

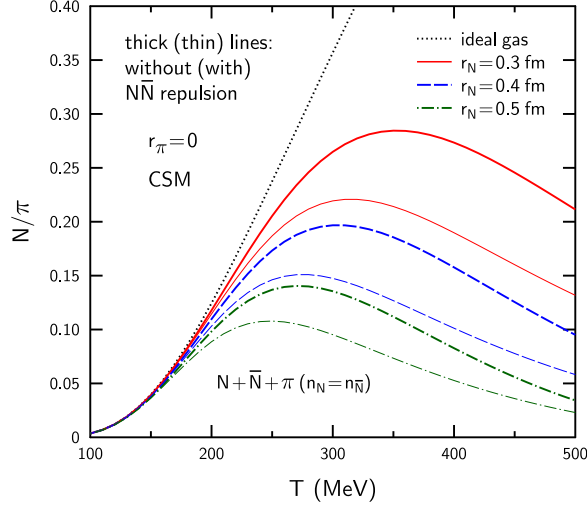


FIG. 4: (Color online) The N/π ratio as a function of temperature in the $N\bar{N}\pi$ matter with equal numbers of nucleons and antinucleons. The thick lines are calculated using the CS approximation of compressibility and disregarding the $N\bar{N}$ interactions. Thin lines give corresponding results with inclusion of the $N\bar{N}$ repulsion. The dotted line is calculated in the ideal gas limit $r_N = 0$.

functions Z and ψ :

$$\frac{P}{T} = 2n_N Z(n_N v_N) + \phi \pi, \quad (38)$$

$$n_N = \phi_N \exp[-\psi(n_N v_N) - \phi \pi v_N], \quad (39)$$

$$n_\pi = \phi_\pi (1 - 2n_N v_N). \quad (40)$$

By comparing Eqs. (36) and (39), one can see that omission of the $N\bar{N}$ repulsion increases the nucleon density at fixed T and r_N . This corresponds to effective reduction of the parameter r_N as compared to standard calculations with equal NN and $N\bar{N}$ interactions.

The results of both calculations are compared in Fig. 4 where the CS approximation of the compressibility factor is used. Note that omitting the $N\bar{N}$ repulsion, indeed, leads to a significant increase of the N/π ratio for large T . Below we extend this analysis to hadronic matter containing heavier hadrons. In particular, we study the sensitivity of the EoS and particle ratios to the omission of the short range repulsion between baryons and antibaryons.

III. HADRON RESONANCE GAS

As already mentioned, the pure $N\bar{N}\pi$ matter is unrealistic at large temperatures and one should take into account excitation of heavier hadrons and hadronic resonances. Note that the presence of resonances in the hadron gas effectively takes into account the attractive interactions of hadrons [28].

In this section we consider the EoS of the $B\bar{B}M$ matter which contains the full set of known baryons (B), antibaryons (\bar{B}) and mesons (M) with masses below 2.6 GeV. Specifically, we use the set of uncharmed hadrons included in the THERMUS model [12]. As before, we neglect the isospin effects and deviations from the Boltzmann statistics. Unless stated otherwise, we apply the zero-width approximation for all hadronic resonances.

One can easily generalize the approach developed in preceding section, assuming that all (anti)baryons have the same hard-core radii, $r_i = r_B$ ($i \in B, \bar{B}$), and all mesons are point-like, $r_i = 0$ ($i \in M$). Below we calculate the total (final) densities of stable hadrons (\bar{n}_i) by including the feeding from strong decays of resonances:

$$\bar{n}_i = n_i + \sum_j n_j Br(j \rightarrow i), \quad (41)$$

where the sum is taken over all resonances. The quantity $Br(j \rightarrow i)$ denotes the average number of i th hadrons from the decays of j th resonance. We calculate these numbers by using the decay tables given in the THERMUS model.

A. Hadronic matter with baryon-antibaryon repulsion

Let us first assume that there is no difference between the BB and $B\bar{B}$ short-range interactions (the corresponding approach will be referred as the CI calculation). Below we denote by $n_B, n_{\bar{B}}$ and n_M the total densities of baryons, antibaryons and mesons, respectively. Applying Eq. (30) for the full set of hadrons, one has

$$\frac{P}{T} = n_T Z(n_T v) + \frac{n_M}{1 - n_T v}, \quad (42)$$

where $n_T = n_B + n_{\bar{B}}$, $v = 4\pi r_B^3/3$ is the hard-core eigenvolume of a baryon, and $Z = Z(\eta)$ is the compressibility factor introduced in Sec. II A.

As shown in Appendix C, Eq. (42) leads to the following expressions for chemical potentials of (anti)baryons and mesons:

$$\frac{\mu_i}{T} = \ln \frac{n_i}{n_i^{\text{id}}} + \psi(n_T v) + \frac{n_M v}{1 - n_T v}, \quad i \in B, \overline{B}, \quad (43)$$

$$\frac{\mu_i}{T} = \ln \frac{n_i}{n_i^{\text{id}}} - \ln(1 - n_T v), \quad i \in M, \quad (44)$$

where n_i^{id} and $\psi(\eta)$ are defined in Eqs. (1) and (6), respectively. Note that first terms in these equations give the chemical potentials of i th hadrons in the ideal gas limit $v \rightarrow 0$.

For the chemically equilibrated matter with zero net baryon charge one has $\mu_i = 0$ for all hadronic species. In this case the relations $n_B = n_{\overline{B}} = n_T/2$ hold. Using further Eqs. (42)–(44) one gets the equations (cf. (35)–(37))

$$\frac{P}{T} = 2n_B Z(2n_B v) + n_M^{\text{id}}, \quad (45)$$

$$n_i = \phi_i \exp[-\psi(2n_B v) - n_M^{\text{id}} v], \quad i \in B, \overline{B}, \quad (46)$$

$$n_i = \phi_i (1 - 2n_B v), \quad i \in M, \quad (47)$$

where $n_M^{\text{id}} = \sum_{i \in M} \phi_i$. Note that the meson component of pressure, given by the last term in the r.h.s. of (45), is the same as in the ideal gas. However, the total pressure and partial densities are reduced due to the interaction of (anti)baryons with mesons. Equations (46) and (47) can be easily solved with respect to n_i . Indeed, taking a sum of both sides of Eq. (46) over all $i \in B$, one gets a single transcendental equation for n_B

$$n_B = n_B^{\text{id}} \exp[-\psi(2n_B v) - n_M^{\text{id}} v], \quad (48)$$

where $n_B^{\text{id}} = \sum_{i \in B} \phi_i$. One can see that solving Eq. (48) is sufficient for calculating pressure and partial densities of all hadrons.

The resulting N/π ratios are presented in Fig. 5. The N/π ratio in the full hadron gas calculation is much smaller than in the $N\overline{N}\pi$ matter. This follows from the fact that the number of additional pions due to decays of meson and baryon resonances is much larger than the corresponding number of nucleons produced in these decays. Evidently, such effects exist already in the ideal gas limit, $r_B \rightarrow 0$ (compare the dotted lines in Fig. 5). As compared to the $N\overline{N}\pi$ matter, the N/π ratio in the full calculation is a much narrower function of T and its maximum is shifted to lower temperatures $T \lesssim 200$ MeV.

The temperature dependence of scaled hadron densities \overline{n}_N and \overline{n}_π (with inclusion of feeding from resonance decays) is given in Fig. 6. One can see that for all temperatures $\overline{n}_N \ll \overline{n}_\pi$.

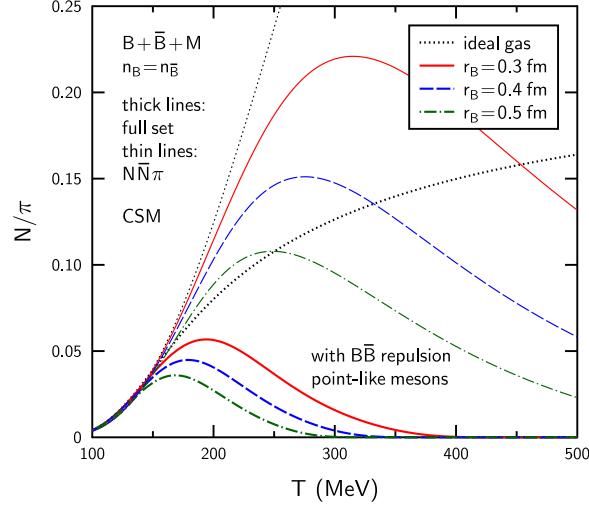


FIG. 5: (Color online) The N/π ratio as a function of temperature in $B\bar{B}M$ matter with point-like mesons. Thick lines show the CSM results for the full set of hadrons with inclusion of feeding from strong decays of resonances (the CI-model). Thin lines are calculated for the $N\bar{N}\pi$ matter. The dotted lines represents the ideal gas limiting case.

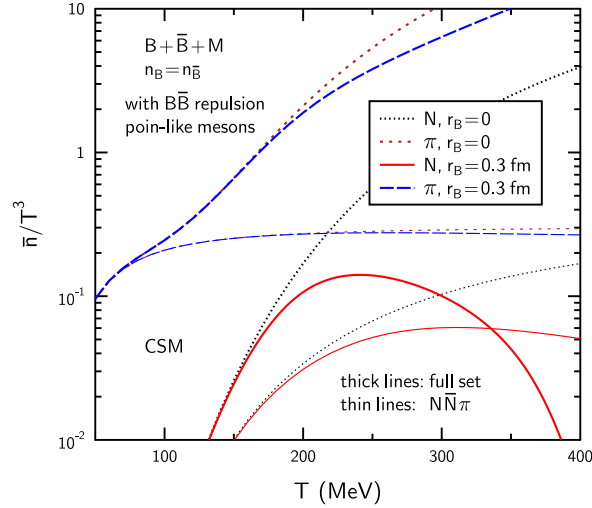


FIG. 6: (Color online) Scaled densities \bar{n}_N/T^3 and \bar{n}_π/T^3 in $B\bar{B}M$ matter with point-like mesons. Thick lines show the CSM results for the full set of hadrons (the CI-model). Thin lines are calculated for the $N\bar{N}\pi$ matter. All calculations correspond to hard-core radius $r_B = 0.3$ fm. The dotted lines represents the ideal gas limiting case.

At $T \gtrsim 100$ MeV, the scaled density \bar{n}_π/T^3 depends only weakly on the temperature for the reduced particle set, but it strongly increases with T in the full hadron gas calculation.

Such a behavior is due to significant excitation of heavy mesons at large temperatures.

B. Hadronic matter without baryon-antibaryon repulsion

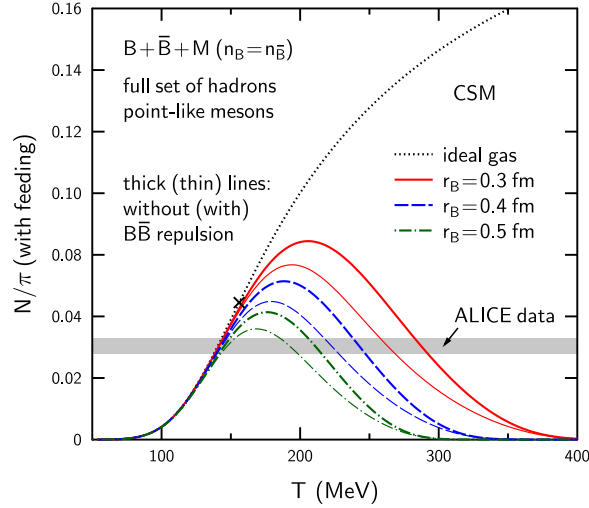


FIG. 7: (Color online) The N/π ratio as a function of temperature in the $B\bar{B}M$ matter (the full set of hadrons) with point-like mesons. Thick (thin) lines show the CSM results within the CII (CI) model. The dotted line represents the ideal gas limiting case. Shading shows experimental bounds for the N/π ratio obtained [29] for 0-5% central Pb+Pb collisions at $\sqrt{s_{NN}} = 2.76$ TeV. The cross represents the N/π value in the ideal gas at $T = 156$ MeV.

Let us consider now matter without $B\bar{B}$ interactions: we refer to this approach as the CII model. As explained in Appendix C, in this case we get the same equations as above, but with the replacement $2n_B \rightarrow n_B$ in the arguments of the functions Z and ψ in Eqs. (45)–(46), (48). Using the same arguments as in Sec. II E one can show that the N/π values should increase in the CII model as compared to the CI calculation. The numerical results presented in Fig. 7 confirm this conclusion. The shaded region in this figure shows the ALICE constraint [29] for central Pb+Pb collisions at the LHC energy. In fact, this Collaboration gives experimental bounds for $(p + \bar{p})/(\pi^+ + \pi^-)$. To get corresponding values of N/π , we introduce the additional factor $2/3$.

Up to now there are no robust estimates of the hard-core radius r_B . It is natural to

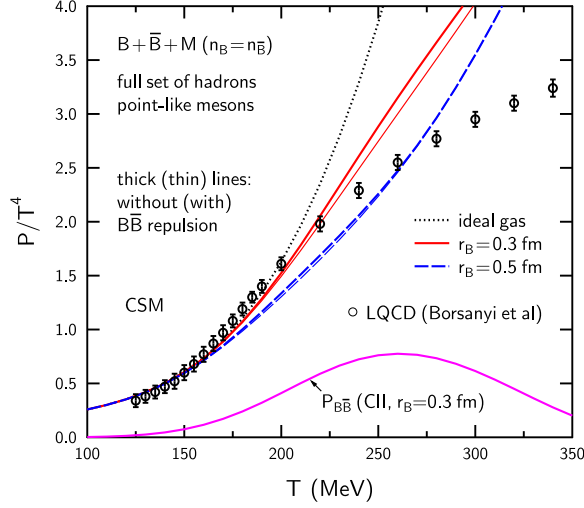


FIG. 8: (Color online) Scaled pressure as a function of temperature in the $B\bar{B}M$ matter (the full set of hadrons) with point-like mesons. Thick (thin) lines show the CSM results within the CII (CI) model. The dotted line represents the ideal gas limiting case. The lower solid curve gives the (anti)baryon part of pressure calculated in the CII model with $r_B = 0.3$ fm. Open dots shows results of lattice QCD calculation [1].

assume that r_B is of the order of the nucleon quark-core radius r_q ⁷. The chiral bag calculations [31, 32] give $r_q \simeq 0.5 - 0.6$ fm. According to our analysis, the N/π values calculated in the CII model meet the experimental constraint for $r_B \lesssim 0.68$ fm⁸. For example, at $r_B = 0.5$ fm the CII-curve in Fig. 7 crosses the "experimental" strip at two temperature intervals: $T = 147 \pm 4$ MeV and $T = 209 \pm 6$ MeV. Note that in the ideal gas limit $r_B \rightarrow 0$ only one (low temperature) interval remains.

The N/π ratio predicted by the ideal gas thermal model [33] for the same reactions corresponds to the point $T = 156$ MeV at the ideal gas curve. This point is marked by a cross in Fig. 7. One can see that the thermal model fit overestimates noticeably the (anti)nucleon-to-pion ratio observed at LHC. Attempts to resolve this discrepancy by introducing the annihilation and regeneration of $B\bar{B}$ pairs at late stages of the reaction have

⁷ We assume that all baryons have approximately same sizes of quark cores. It is argued in Ref. [30] that repulsion between baryons at small distances $r < 2r_q$ appears due to the Pauli principle which prevents identical fermions (quarks) to overlap in the phase space.

⁸ At larger r_B the calculated N/π values are below the shaded region in Fig. 7. The corresponding condition for the CI-case is $r_B \lesssim 0.62$ fm.

been made in Refs. [34, 35].

In Fig. 8 we compare the results of pressure calculations within the CI and CII models with the lattice QCD data. One can see these two models predict rather similar results. The low sensitivity of pressure to the omission of $B\bar{B}$ repulsion is explained by a relatively small contribution of (anti)baryons (the first term of Eq. (45)) as compared to mesons.

C. Hadronic matter without (anti)baryon-meson repulsion

Up to now we described the MB and $M\bar{B}$ interactions in the excluded volume scenario: it was assumed that point-like mesons do not penetrate into the volume occupied by hard-cores of (anti)baryons. In this approximation interactions of (anti)baryons with mesons lead to additional shifts of chemical potentials given by the last terms in Eqs. (43) and (44). One should have in mind, that such a purely classical picture is especially questionable for pion interactions. Indeed, at $T \gtrsim m_\pi$ the thermal wave length of pions is of the order of T^{-1} . At $T \lesssim 400$ MeV this length is at least comparable with typical hardcore radii of baryons.

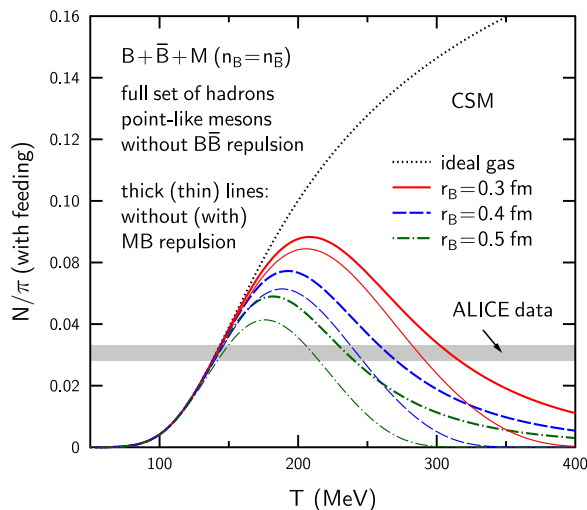


FIG. 9: (Color online) The ratio N/π as a function of temperature in the $B\bar{B}M$ matter (the full set of hadrons) with point-like mesons. Thick (thin) lines show the CSM results within the CIII (CII) model. The dotted line represents the ideal gas limiting case. Shading shows experimental bounds for the N/π ratio obtained [29] for 0-5% central Pb+Pb collisions at $\sqrt{s_{NN}} = 2.76$ TeV.

Quantum calculations of the second virial coefficients have been performed earlier for purely pion [27] and πNK [28] matter. These coefficients were expressed via the momentum

integrals of phenomenological phase shifts of binary hadronic scattering. It was shown that the repulsive and attractive contributions nearly cancel for pion interactions. Qualitatively, such interactions may be described by the addition of meson and baryon resonances⁹. Interactions of heavier mesons are, presumably, less modified due to quantum effects. Note that the role of Pauli suppression for short-range interactions of mesons with (anti)baryons should be less significant as compared to BB and $\overline{B}\overline{B}$ pairs.

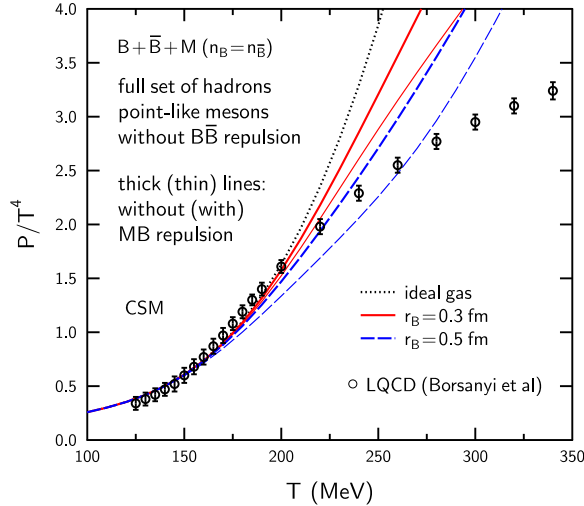


FIG. 10: (Color online) Scaled pressure as a function of temperature in the $B\overline{B}M$ matter (the full set of hadrons) with point-like mesons. Thick (thin) lines show the CSM results within the CII (CIII) model. The dotted line represents the ideal gas limiting case. Open dots shows results of lattice QCD calculation [1].

This discussion shows that one can expect reduced MB and $M\overline{B}$ short-range interactions as compared to a simple classical scenario. To estimate the role of such interactions, we modify the CII calculation, by omitting additionally the MB and $M\overline{B}$ short-range repulsion for all mesons. In this new scenario (the CIII model) mesons can be considered as an ideal gas, with partial densities $n_i = \phi_i$ ($i \in M$). Omitting denominators in Eqs. (42)–(43) and applying the procedure similar to those used in Sec. III A we get the relations

$$\frac{P}{T} = 2n_B Z(n_B v) + n_M^{\text{id}}, \quad (49)$$

$$n_i = \phi_i \exp[-\psi(n_B v)], \quad i \in B, \overline{B}, \quad (50)$$

⁹ Note that this conclusion is obtained only for second-order virial coefficients and therefore, it may be not valid for high-order terms.

where n_B is determined by solving the equation $n_B = n_B^{\text{id}} \exp[-\psi(n_B v)]$. It is clear that the hadron densities and pressure increase in the new scenario as compared to the CII model.

Comparison of CII and CIII calculations is given in Figs. 9 and 10. It is seen that the N/π ratio increases and becomes a broader function of temperature in the CIII model. These effects are more significant at larger r_B . According to Fig. 10, the pressure is closer to the ideal gas in the new calculation, especially at large temperatures. It is important that at $r_B \sim 0.5$ fm the lattice QCD data are satisfactory reproduced in the CIII model at $T \lesssim 250$ GeV.

IV. FITTING THE ALICE HADRON YIELDS IN PB+PB COLLISIONS

In this section we perform the fit to the midrapidity yields of hadrons $\pi^\pm, K^\pm, K_S^0, p, \bar{p}, \Lambda, \Xi^\pm, \Omega^\pm$, and ϕ measured by the ALICE collaboration in the 0 – 5% central Pb+Pb collisions at $\sqrt{s_{NN}} = 2.76$ TeV [37]¹⁰. We perform the fits for the ideal hadron gas as well as for the CI, CII, and CIII models, introduced in Sec. III. In these calculations nonzero mass widths of resonances are taken into account (for details, see Ref. [17]). The baryon compressibility factor Z is chosen in the excluded volume form (3), and all mesons are considered as point-like particles.

At the LHC energies the asymmetry in the production of particles and antiparticles becomes negligible. This implies nearly zero values of all chemical potentials in a statistical system. The hadron yield ratios would then be determined by a single free parameter – the so called chemical freeze-out temperature T . The statistical quality of such a fit is defined by the value of χ^2/N_{dof} . Figure 11 shows the temperature dependence of χ^2/N_{dof} for the ideal gas (dotted lines), as well as for the models CI, CII, and CIII. The results with hard-core baryon radii $r_B = 0.3, 0.4, 0.5$, and 0.6 fm are presented in the panels (a), (b), (c), and (d), respectively. In all models, at each temperature, the only remaining free parameter is the system volume. In fitting the midrapidity hadron yields, this parameter is fixed at each T to minimize the χ^2 values of the fit. The best fit for each model corresponds to the minimum χ^2/N_{dof} value.

¹⁰ Note that the centrality binning for Ξ and Ω hyperons is different from other hadrons in the ALICE experiments. Thus, we take the midrapidity yields of Ξ and Ω in the 0 – 5% centrality class from Ref. [38], where they were obtained using the interpolation procedure.

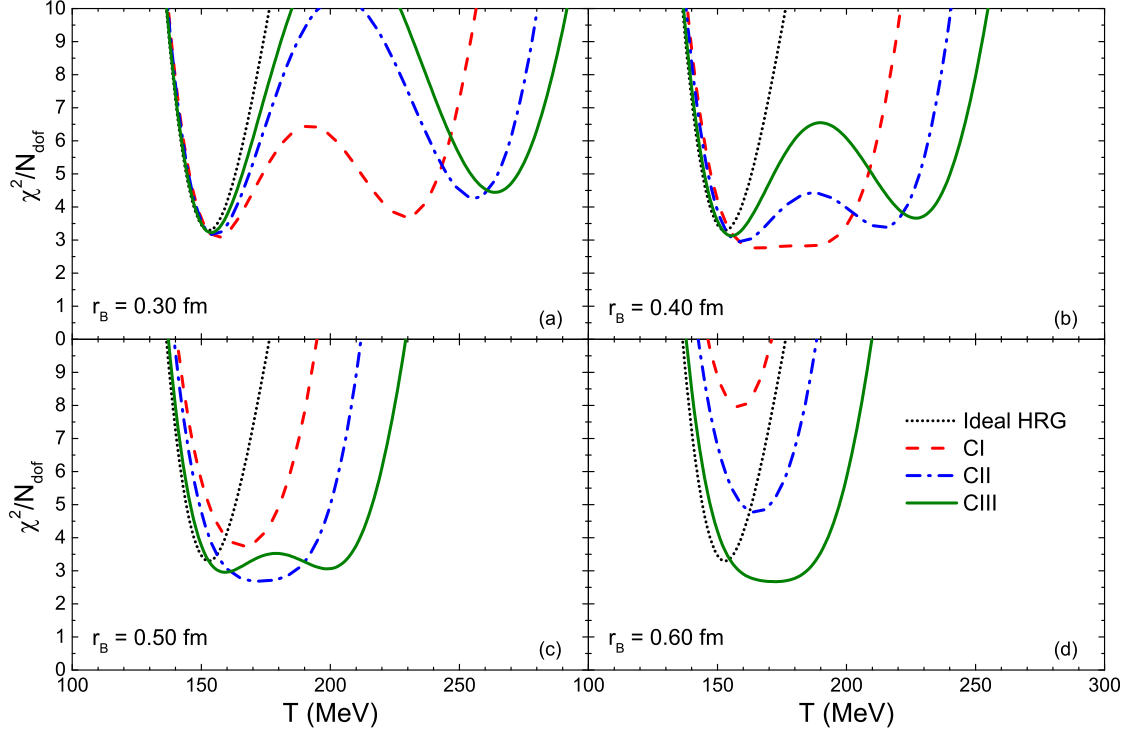


FIG. 11: (Color online) The temperature dependence of χ^2/N_{dof} for fitting the ALICE data on hadron yields in 0-5% central Pb+Pb collisions at $\sqrt{s_{NN}} = 2.76$ TeV. The dashed, dash-dotted, and solid curves correspond, respectively, to the models CI, CII, and CIII. The dotted lines are calculated in the ideal gas limit $r_B = 0$.

Two important features of the results shown in Fig. 11 should be pointed out. First, introducing non-zero hard-core radii for baryons increases the chemical freeze-out temperature (i.e. shifts the position of the χ^2/N_{dof} minimum to the right) and improves the fit's quality (reduces the minimum value of χ^2/N_{dof}). Second, the structure of the χ^2/N_{dof} curves as a function of T in the models CI, CII, and CIII is very different as compared to the ideal gas case. The corresponding curves are noticeably wider, and in many cases two minima appear. Therefore, extracting the chemical freeze-out temperature from the hadron yield data is a rather delicate procedure: it strongly depends on details of the model for the short-range repulsion and on the choice of hard-core radii of baryons. One can see a significant difference between the CI and CII results. This shows that improved excluded volume models should take into account the difference between the BB and $B\bar{B}$ interactions. Introducing non-zero hard-core radii for mesons $r_M < r_B$ within the NDEM can improve both the quality of fitting the observed hadron yields and the agreement with the lattice QCD data at $T \sim 200$ MeV.

V. CONCLUSIONS AND OUTLOOK

Modeling the short-range interactions in the hadronic gas remains an open problem. For a simple system of finite-size (anti)baryons and point-like mesons, here several different formulations (e.g., CI, CII, and CIII) are analyzed. Omission of meson–baryon and antibaryon–baryon interactions strongly influences the pressure and hadronic densities.

Similar to Ref. [17] it is found that commonly used diagonal eigenvolume models are not realistic for quantitative studies, especially in the situation when hard-core radii of mesons are significantly smaller than those for (anti)baryons.

The nucleon-to-pion ratio in hadronic gas is a non-monotonic function of temperature. This increases uncertainties in attempts to extract the freeze-out temperature by fitting the hadronic ratios observed in heavy-ion collisions. This also explains the appearance of the second, high-temperature minimum of χ^2 distribution obtained from the thermal fit of ALICE data in Ref. [16].

We show that more refined formulations of the eigenvolume model (e.g. the Carnahan-Starling one) give similar results for baryon-symmetric matter as compared to the simple van der Waals approach.

Simultaneous description of the observed hadron ratios and lattice QCD data for the pressure, energy density, as well as fluctuations of conserved charges may help in studying the role of short-range interactions in hadronic matter. Of course, the transition region between the fully confined hadronic phase and the deconfined matter should be taken into account at high enough temperatures. To take these effects into account, one can use the approach suggested in Ref. [36]. In this scheme a crossover EoS has been suggested which interpolates the hadron gas phase with excluded volume corrections and the deconfined states in a perturbative QCD model.

Acknowledgments

The authors thank K. A. Bugaev, I. N. Mishustin, and P. M. Lo for useful discussions. A partial support from the grant NSH–932.2014.2 of the Russian Ministry of Education and Science is acknowledged by L.M.S. The work of M.I.G. is supported by the Goal-Oriented Program of the National Academy of Sciences of Ukraine and the European Organization

for Nuclear Research (CERN), Grant CO-1-3-2016, and by the Program of Fundamental Research of the Department of Physics and Astronomy of National Academy of Sciences of Ukraine.

Appendix A

Since the particle numbers are not fixed in the equilibrium hadronic matter, it is natural to describe its properties in the grand canonical variables. On the other hand, the hard-sphere interactions are easier introduced in the CE. Below we apply a rather general algorithm of transition to the GCE suggested in Refs. [20, 39]. An equivalent procedure has been used in [40, 41].

Let us assume that one knows pressure P in the CE, i.e. as a function of temperature and partial densities n_i . Then one can easily calculate the free energy density $f = F/V = f(T, n_1, n_2, \dots)$ for arbitrary multiparticle interactions (see below). This quantity is a genuine thermodynamical potential in the CE. One can write the thermodynamic relation [18]:

$$f = \sum_i \mu_i n_i - P, \quad (\text{A1})$$

where $\mu_i = (\partial f / \partial n_i)_T$ is the i th particle chemical potential and the sum goes over all particle species i . In the limit of ideal Boltzmann gas one has the following relations for thermodynamic functions in the CE (see Eq. (1))

$$P^{\text{id}} = T \sum_i n_i, \quad \mu_i^{\text{id}} = T \ln \frac{n_i}{\phi_i}, \quad f^{\text{id}} = T \sum_i n_i \left(\ln \frac{n_i}{\phi_i} - 1 \right). \quad (\text{A2})$$

Here the last equality follows from Eq. (A1).

Particle interactions give rise to nonzero shifts of the free energy density, $\Delta f = f - f^{\text{id}}$, and pressure, $\Delta P = P - P^{\text{id}}$, with respect to the ideal gas. One can use the relation $dF = PdV$ for the free energy change in the isothermal process. Taking the integral over the system volume V (at fixed particle multiplicities $N_i = n_i V$), we get the equation [20]

$$\Delta f(T, n_1, n_2, \dots) = \int_0^1 \frac{d\alpha}{\alpha^2} \Delta P(T, \alpha n_1, \alpha n_2, \dots). \quad (\text{A3})$$

Finally, the free energy density is found from $f = f^{\text{id}} + \Delta f$.

Let us consider first the one-component matter with hard-sphere interactions. In accordance with Eq. (2) one has $\Delta P(T, n) = nT [Z(nv) - 1]$, where v is the hard-core volume of a single particle. Substituting this expression into (A3) one obtains

$$\Delta f(T, n) = nT \int_0^{nv} \frac{d\eta}{\eta} [Z(\eta) - 1]. \quad (\text{A4})$$

Taking further the density derivative, one gets the following expression for the shift of chemical potential:

$$\Delta\mu = \left(\frac{\partial \Delta f}{\partial n} \right)_T = T\psi(nv), \quad (\text{A5})$$

where $\psi(\eta)$ is defined in Eq. (6). One can see, that $T\psi(\eta)$ gives the chemical potential shift for a one-component gas with the packing fraction $\eta = nv$. Formally, this shift can be described by introducing the repulsive mean-field potential $U(T, n) = T\psi(nv)$ [21]. Adding the ideal gas chemical potential (see Eq. (A2)) gives [20]

$$\mu = T \left[\ln \frac{n}{\phi(T)} + \psi(nv) \right]. \quad (\text{A6})$$

This formula can be written in the form $n = n^{\text{id}}(T, \mu - \Delta\mu)$, which is in turn equivalent to Eq. (5) of the main text. Finally, pressure $P = P(T, \mu)$ in the GCE is obtained by substituting in (2) the solution of Eq. (A6) with respect to n .

By using Eq. (7) one can show that Eq. (A6) leads to the following equation for pressure in the EVM:

$$P = P^{\text{id}}(T, \mu - bP), \quad (\text{A7})$$

where $b = 4v$ and $P^{\text{id}}(T, \mu) = T\phi(T) \exp(\mu/T)$. Note that this model becomes inaccurate at densities $n \gtrsim 0.2/v$.

Let us now consider the GCE formulation of the DEM introduced in Sec. II B. Substituting $\Delta P = T \sum_i n_i \left[(1 - \sum_j b_j n_j)^{-1} - 1 \right]$ into Eq. (A4) gives the relations

$$\Delta f = T \sum_i n_i \ln \frac{\xi_i}{n_i}, \quad (\text{A8})$$

$$\Delta\mu_i = \left(\frac{\partial \Delta f}{\partial n_i} \right)_T = T \ln \frac{\xi_i}{n_i} + b_i P. \quad (\text{A9})$$

Adding the ideal gas chemical potential from Eq. (A2) gives Eq. (10) of the main text.

A similar transition algorithm can be developed in the NDEM. Starting from Eq. (24) and calculating the integral in Eq. (A3), one obtains the relations (25) and (26).

Appendix B

Let us consider a two-component matter composed of particles with hard-core radii r_1, r_2 and assume that $r_2 = 0$. The EoS for such matter in the canonical variables T, n_1, n_2 is given by Eq. (30). We use a general form of the compressibility factor for the first component $Z = Z(\eta_1)$, where $\eta_1 = n_1 v_1$ and $v_1 = 4\pi r_1^3/3$. The results in the EVM and CSM are obtained after substituting $Z = Z_{\text{EV}}$ and $Z = Z_{\text{CS}}$, respectively.

Using Eqs. (30) and (A3) one gets the relation for the free energy shift

$$\Delta f = T n_1 \int_0^{\eta_1} \frac{d\eta}{\eta} [Z(\eta) - 1] - T n_2 \ln(1 - \eta_1). \quad (\text{B1})$$

This equation leads to the following formulae for shifts of chemical potentials:

$$\Delta \mu_1 = \left(\frac{\partial \Delta f}{\partial n_1} \right)_T = T \left[\psi(\eta_1) + \frac{n_2 v_1}{1 - \eta_1} \right], \quad (\text{B2})$$

$$\Delta \mu_2 = \left(\frac{\partial \Delta f}{\partial n_2} \right)_T = -T \ln(1 - \eta_1). \quad (\text{B3})$$

Adding the ideal gas chemical potentials $\mu_i^{\text{id}} = T \ln(n_i/\phi_i)$ gives Eqs. (31) and (32) of the main text.

Appendix C

Let us consider the hadronic matter with hard-sphere interactions and assume that all (anti)baryons has the same hard-core radii r_B , but mesons are point-like. We start from the CI model which does not distinguish the BB and $B\bar{B}$ interactions. In this case using Eq. (42) leads to the relation

$$\Delta P = P - (n_T + n_M)T = T n_T [Z(n_T v) - 1] + T n_M [(1 - n_T v)^{-1} - 1]. \quad (\text{C1})$$

Calculating the integral in (A3) and using (6) give the following expression for the free energy density:

$$\begin{aligned} f = f^{\text{id}} + \Delta f = T \sum_{i \in B, \bar{B}, M} n_i \left[\ln \frac{n_i}{\phi_i} - 1 \right] \\ + T n_T [\psi(n_T v) - Z(n_T v) + 1] - T n_M \ln(1 - n_T v). \end{aligned} \quad (\text{C2})$$

The first terms in this equation give the free energy density of the ideal hadronic gas. Taking the derivative of (C2) with respect to n_i one obtains Eqs. (43) and (44) for chemical potentials.

Analogous formulae for the CII model (without the baryon-antibaryon repulsion) are given by Eqs. (C1) and (C2), with the replacements

$$n_T Z(n_T v) \rightarrow n_B Z(n_B v) + n_{\bar{B}} Z(n_{\bar{B}} v), \quad (\text{C3})$$

$$n_T \psi(n_T v) \rightarrow n_B \psi(n_B v) + n_{\bar{B}} \psi(n_{\bar{B}} v). \quad (\text{C4})$$

In this case one obtains the same equations (45)–(48), but with the replacement $2n_B \rightarrow n_B$ in the arguments of functions Z and ψ .

-
- [1] Sz. Borsányi, Z. Fodor, C. Hoelbling, S. D. Katz, S. Krieg and K. K. Szabó, Phys. Lett. B **730**, 99 (2014).
 - [2] A. Bazavov *et al.* [Hot QCD Collaboration], Phys. Rev. D **90**, 094503 (2014).
 - [3] D. H. Rischke, M. I. Gorenstein, H. Stoecker, and W. Greiner, Z. Phys. C: Part. Fields **51**, 485 (1991).
 - [4] L. M. Satarov, M. N. Dmitriev, and I. N. Mishustin, Phys. Atom. Nucl. **72**, 1390 (2009).
 - [5] H. Stoecker, A. A. Ogloblin, and W. Greiner, Z. Phys. A **303**, 259 (1981).
 - [6] D. Hahn and H. Stoecker, Phys. Rev. C **35**, 1311 (1987).
 - [7] J. Cleymans and H. Satz, Z. Phys. C: Part. Fields **57**, 135 (1993).
 - [8] P. Braun-Munzinger and J. Stachel, Nucl. Phys. A **606**, 320 (1996).
 - [9] F. Becattini, J. Cleymans, A. Keranen, E. Suhonen, and K. Redlich, Phys. Rev. C **64**, 024901 (2001).
 - [10] J. Cleymans, K. Redlich, H. Satz, and E. Suhonen, Z. Phys. C: Part. Fields **33**, 151 (1986).
 - [11] G. D. Yen, M. I. Gorenstein, W. Greiner, and S. N. Yang, Phys. Rev. C **56**, 2210 (1997);
G. D. Yen and M. I. Gorenstein, Phys. Rev. C **59**, 2788 (1999).
 - [12] S. Wheaton, J. Cleymans, M. Hauer, Comput. Phys. Commun. **180**, 84 (2009).
 - [13] M. I. Gorenstein, A. P. Kostyuk, and Y. D. Krivenko, J. Phys. G: Nucl. Part. Phys. **25**, L75 (1999).
 - [14] K. A. Bugaev *et al.*, Eur. Phys. Lett. **104**, 22002 (2013).

- [15] K. A. Bugaev, D. R. Oliinychenko, A. S. Sorin, and G. M. Zinovjev,
Eur. Phys. J. A **49**, 30 (2013).
- [16] V. Vovchenko and H. Stoecker, arXiv: 1512.08046 [hep-ph].
- [17] V. Vovchenko and H. Stoecker, arXiv: 1606.06218 [hep-ph].
- [18] L. D. Landau and E. M. Lifshitz, *Statistical Physics* (Oxford: Pergamon) 1975.
- [19] N. F. Carnahan and K. E. Starling, J. Chem. Phys. **51**, 635 (1969).
- [20] L. M. Satarov, K. A. Bugaev, and I. N. Mishustin, Phys. Rev. C **91**, 055203 (2015).
- [21] D. Anchishkin, V. Vovchenko, J. Phys. G: Nucl. Part. Phys. **42**, 105102 (2015).
- [22] E. Klempt, F. Bradamante, A. Martin, J.-M. Richard, Phys. Rep. **368**, 119 (2002).
- [23] *Theory and Simulation of Hard Sphere Fluids and Related Systems*,
Lect. Notes Phys. vol. 753, ed. by A. Mulero (Springer-Verlag, Berlin, 2008).
- [24] A. Mulero, C. A. Faúndez, and P. Cuadros, Mol. Phys. **97**, 453 (1999).
- [25] I. N. Mishustin, L. M. Satarov, T. J. Bürvenich, H. Stoecker, and W. Greiner,
Phys. Rev. C **71**, 035201 (2005).
- [26] A. Andronic, P. Braun-Munzinger, J. Stachel, M. Winn, Phys. Lett. B **718**, 80 (2012).
- [27] A. Kostyuk, M. Gorenstein, H. Stoecker, and W. Greiner, Phys. Rev. C **63**, 044901 (2001).
- [28] R. Venugopalan and M. Prakash, Nucl. Phys. A **546**, 718 (1992).
- [29] B. Abelev *et al.* [ALICE Collaboration], Phys. Rev. Lett. **109**, 252301 (2012).
- [30] V. G. Neudachin, I. T. Obuhovsky, V. K. Kukulin, and N. F. Golovanova,
Phys. Rev. C **11**, 128 (1975).
- [31] R. Tegen, M. Schedl and W. Weise, Phys. Lett. B **125**, 9 (1983).
- [32] F. Myhrer, J. Wroldsen, Rev. Mod. Phys. **60**, 629 (1988).
- [33] P. Braun-Munzinger, V. Koch, T. Schäfer, J. Stachel, Phys. Rep. **621**, 76 (2016).
- [34] L. M. Satarov, I. N. Mishustin, and W. Greiner, Phys. Rev. C **88**, 024908 (2013).
- [35] Y. Pan, S. Pratt, Phys. Rev. C **89**, 044911 (2014).
- [36] M. Albright, J. Kapusta, C. Young, Phys. Rev. C **90**, 024915 (2014).
- [37] B. Abelev *et al.* [ALICE Collaboration], Phys. Rev. C **88**, 044910 (2013);
B. B. Abelev *et al.* [ALICE Collaboration], Phys. Rev. Lett. **111**, 222301 (2013);
B. B. Abelev *et al.* [ALICE Collaboration], Phys. Lett. B **728**, 216 (2014);
B. B. Abelev *et al.* [ALICE Collaboration], Phys. Rev. C **91**, 024609 (2015).
- [38] F. Becattini, E. Grossi, M. Bleicher, J. Steinheimer, and R. Stock,

- Phys. Rev. C **90**, 054907 (2014).
- [39] B. J. Alder, J. Chem. Phys. **23**, 263 (1955).
- [40] V. Vovchenko, D. V. Anchishkin, and M. I. Gorenstein,
J. Phys. A: Math. Theor. **48**, 305001 (2015).
- [41] K. Redlich, K. Zalewski, Acta Phys. Polon. B **47**, 1943 (2016).